Molecular Modeling and Site-Directed Mutagenesis Reveal Essential Residues for Catalysis in a Prokaryote-Type Aspartate Aminotransferase[1][W][OA]

Fernando de la Torre[2], Aurelio A. Moya-García[2], María-Fernanda Suárez, Carlos Rodríguez-Caso, Rafael A. Cañas, Francisca Sánchez-Jiménez, and Francisco M. Cánovas*

Departamento de Biología Molecular y Bioquímica and Instituto Andaluz de Biotecnología (F.d.l.T., M.-F.S., R.A.C., F.M.C.) and Departamento de Biología Molecular y Bioquímica and Centro de Investigación Biomédica en Red de Enfermedades Raras (A.A.M.-G., C.R.-C., F.S.-J.), Campus Universitario de Teatinos, Universidad de Málaga, 29071 Málaga, Spain

We recently reported that aspartate (Asp) biosynthesis in plant chloroplasts is catalyzed by two different Asp aminotransferases (AAT): a previously characterized eukaryote type and a prokaryote type (PT-AAT) similar to bacterial and archaebacterial enzymes. The available molecular and kinetic data suggest that the eukaryote-type AAT is involved in the shuttling of reducing equivalents through the plastidic membrane, whereas the PT-AAT could be involved in the biosynthesis of the Asp-derived amino acids inside the organelle. In this work, a comparative modeling of the PT-AAT enzyme from *Pinus pinaster* (PpAAT) was performed using x-ray structures of a bacterial AAT (*Thermus thermophilus*; Protein Data Bank accession nos. 1BJW and 1BKG) as templates. We computed a three-dimensional folding model of this plant homodimeric enzyme that has been used to investigate the functional importance of key amino acid residues in its active center. The overall structure of the model is similar to the one described for other AAT enzymes, from eukaryotic and prokaryotic sources, with two equivalent active sites each formed by residues of both subunits of the homodimer. Moreover, PpAAT monomers folded into one large and one small domain. However, PpAAT enzyme showed unique structural and functional characteristics that have been specifically described in the AATs from the prokaryotes *Phormidium lapideum* and *T. thermophilus*, such as those involved in the recognition of the substrate side chain or the "open-to-closed" transition following substrate binding. These predicted characteristics have been substantiated by site-direct mutagenesis analyses, and several critical residues (valine-206, serine-207, glutamine-346, glutamate-210, and phenylalanine-450) were identified and functionally characterized. The reported data represent a valuable resource to understand the function of this enzyme in plant amino acid metabolism.

Aspartate aminotransferase (AAT; Asp:2-oxoglutarate aminotransferase; EC 2.6.1.1) catalyzes the reversible transamination reaction between Asp and 2-oxoglutarate to give Glu and oxaloacetate via a ping-pong bi-bi mechanism. AAT enzymes have been classified into the aminotransferase family I and then divided into two subfamilies, Iα and Iβ, according to their amino acid sequence identities (Jensen and Gu, 1996). To date, subfamily Iα includes AATs from eubacteria and eukaryotes, while subfamily Iβ includes those from bacteria and archaea. The amino acid sequence identities between members of subfamily Iα (about 40%) is slightly higher than the identities between members of subfamily Iβ (30%–35%). When Iα and Iβ sequences are compared, only about 15% identity can be observed.

Many x-ray crystallographic studies have been performed on enzymes of subfamily Iα to elucidate their structure, function, and catalytic mechanism. These include AATs from *Escherichia coli* (Okamoto et al., 1994), chicken (Malashkevich et al., 1995), and pig (Rhee et al., 1997). These studies showed that all of these enzymes have a very similar three-dimensional (3D) structures and the same homodimeric quaternary structure, consisting of identical monomers with a molecular size of about 45 kD (Kallen et al., 1985). Each polypeptide chain is folded into a large domain and a small domain on the basis of the correlated motion of the N-terminal and C-terminal parts of the polypeptide chain upon inhibitor binding. The active site pocket is located at the interface between both domains. The pyridoxal-phosphate (PLP) coenzyme resides at the bottom of the active site and forms a Schiff base with a Lys residue. A large conformational

[1] This work was supported by the Ministerio de Ciencia e Innovación, Spain (grant no. BIO2006–06216), and the Junta de Andalucía (grant nos. P05–AGR663 and P08–CVI02999 and research groups BIO–114 and BIO–267). This work is part of the activities of the Andalusian platform for Genomics, Proteomics, and Bioinformatics.

[2] These authors contributed equally to the article.

* Corresponding author; e-mail canovas@uma.es.

The author responsible for distribution of materials integral to the findings presented in this article in accordance with the policy described in the Instructions for Authors (www.plantphysiol.org) is: Francisco M. Cánovas (canovas@uma.es).

[W] The online version of this article contains Web-only data.

[OA] Open Access articles can be viewed online without a subscription.

www.plantphysiol.org/cgi/doi/10.1104/pp.108.134510

change in the small domain toward the large domain (from open to closed form) has been well described in the AAT subfamily Iα, which occurs when a C4 dicarboxylic substrate (Asp) binds close to the active site of the enzyme (McPhalen et al., 1992; Jäger et al., 1994; Okamoto et al., 1994). That means that the catalytic AAT reaction proceeds in the closed structure of the enzyme when Asp is transaminated to 2-oxoglutarate. The closed structure is maintained by electrostatic and hydrophobic interactions between residues located in the active site and the substrate. Recently, a detailed analysis of the AAT structure for the reverse reaction using C5 dicarboxylic substrates suggested that the Michaelis complex with Glu instead of Asp presents the open conformation (Islam et al., 2005). Interestingly, a very similar 3D structure, based on x-ray crystallography, has been observed for AAT members of subfamily Iβ analyzed by x-ray (Nakai et al., 1998; Kim et al., 2003; PDB 1J32), despite the observed divergence in primary structures. In the AAT of *Thermus thermophilus* HB8 (ttAAT), a member of subfamily Iβ, a large conformational change from the open to the closed form has been described (Nakai et al., 1999).

Amino acid sequence comparison clearly shows that critical residues in the active site are conserved in all AAT enzymes belonging to subfamily Iα. When the primary structure of AAT enzymes from subfamilies Iα and Iβ are compared, most of the residues that are involved in the active site and that are essential for the catalytic mechanism seem to be conserved, despite the low identity between both AAT types (Nakai et al., 1999). Single residues are implicated in the catalytic mechanism along with other essential residues that are not conserved in subfamily Iβ. An example is the amino acid Arg-292, which is involved in the recognition of the distal carboxylate of the Asp substrate in subfamily Iα. In subfamily Iβ, the same role seems to be carried out by the Lys-109 residue (Nobe et al., 1998).

The AAT enzyme is present in plants as a family composed of at least five different isoenzymes associated with different subcellular compartments (cytosol, chloroplast, mitochondria, and peroxisome). An increasing number of cDNA sequences encoding AAT isoenzymes have been reported in different plants, such as alfalfa (*Medicago sativa*; Gantt et al., 1992), Arabidopsis (*Arabidopsis thaliana*; Schultz and Coruzzi, 1995; Wilkie et al., 1995), broomcorn millet (*Panicum miliaceum*; Taniguchi et al., 1995), carrot (*Daucus carota*; Turano et al., 1992), lupine (*Lupinus albus*; Reynolds et al., 1992), and soybean (*Glycine max*; Wadsworth et al., 1993). Comparative analysis of amino acid sequences indicates that plant AAT isoenzymes are in the same protein family as the vertebrate AATs and bacterial AATs of subfamily Iα (Wadsworth, 1997). No x-ray crystallographic studies for any plant AAT have been performed. Furthermore, only one protein structure has been modeled (Wilkie et al., 1996), the plastidic isoform of eukaryote-type AAT from Arabidopsis, which is encoded by the At4g31990 locus.

We recently reported the existence in plants of a novel form of AAT (prokaryote-type AAT [PT-AAT]) with a high degree of similarity to the enzymes from cyanobacteria and archaea (de la Torre et al., 2006, 2007). This finding constitutes the first evidence, to our knowledge, of AAT belonging to subfamily Iβ in eukaryotic organisms. The gene encoding PT-AAT is highly expressed in photosynthetically active tissues, and the enzyme is located in the chloroplast. A putative endosymbiotic origin has been proposed for this enzyme based on its subcellular localization and sequence similarities. The aim of this investigation is to find out the differential role of this PT-AAT with regard to the already described members of the plant AAT gene family. Structural modeling of the enzyme from *Pinus pinaster* (PpAAT) and site-direct mutagenesis experiments should help in understanding the role of critical residues and the mechanism of interaction between substrate and enzyme. Knowledge of the structural and functional characteristics of this novel plant enzyme represents a valuable resource to gain further insights into its function in plant amino acid metabolism.

RESULTS

Amino Acid Sequence Comparison between Plant PT-AAT and Bacterial and Eukaryotic AATs

Nucleotide and protein databases reveal the existence in plants of two types of AAT enzymes. The first type corresponds to the eukaryote-type Iα, which is also found in animals and some eubacteria. The second type, composed solely of a single member in plants, corresponds to the prokaryotic type (de la Torre et al., 2006) and belongs to subfamily Iβ of AATs. Numerous full-length sequences corresponding to type Iβ AAT have previously been characterized in different species of cyanobacteria and other prokaryotes, such as *Phormidium lapideum* (accession no. AB063283.1), *Prochlorococcus marinus* (BX572097.1), *Anabaena variabilis* (CP000117.1), *Thermosynechococcus elongatus* BP-1 (NP_683147), and *T. thermophilus* (NC005835.1). By contrast, only four full-length sequences belonging to type Iβ are available in plants (de la Torre et al., 2006). These are in Arabidopsis (AY064152.1), *Oryza sativa* (AP003235.2), *P. pinaster* (AJ 628016.1), and *Populus trichocarpa* (Poptr1: 695900). Nevertheless, similar gene sequences are present in the genomes of *Vitis vinifera* and *Carica papaya*, and partial sequences with a high level of identity have been identified in the public databases for the ongoing genome projects of tomato (*Solanum lycopersicum*; sgn.cornell.edu) and maize (*Zea mays*; www.maizegdb.org).

Previous multiple alignments built with AAT sequences from distant species have highlighted a few evolutionarily conserved residues. Thus, most of the residues described as essential to carry out the enzymatic reactions are conserved between enzymes be-

longing to the Iα and Iβ subfamilies (de la Torre et al., 2006). The alignment represented in Figure 1 compares the primary structures of different PT-AATs with bacterial (*T. thermophilus*) and eukaryotic (*Sus scrofa*) AAT models. Protein sequences for plant AATs, including the chloroplast transit peptide, were aligned, revealing that the plant PT-AATs are well-conserved enzymes (74%–77% identity) and show a remarkably high level of identity with the bacteria-type Iβ AATs (37%–45% identity). However, many residues that are completely conserved in the plant sequences are not present in the bacterial AAT. Furthermore, a stretch of 11 amino acids in the plant polypeptides (positions 421–432 in the pine sequence) is absent in the *T. thermophilus* protein sequence (Fig. 1). In addition, the plant PT-AATs and eukaryote-type AATs are unrelated enzymes (Fig. 1).

Computer Modeling of the Structure of PpAAT

The amino acid sequences of PpAAT and other members of subfamily Iβ for which 3D structures are known (Nakai et al., 1998; Kim et al., 2003) were compared. It was found that the AAT enzymes from the cyanobacteria *P. lapideum* (plAAT) and from *T. thermophilus* (ttAAT) are 45% and 42% identical to PpAAT, respectively. Since the ttAAT structure has been resolved in both open and closed conformations, it was selected as a template for the protein modeling of PpAAT. The accuracy of comparative models decreases sharply below the 30% sequence identity cutoff, mainly as a result of a rapid increase in alignment errors (Madhusudhan et al., 2005). Since the sequence identity between ttAAT and PpAAT is 42%, we are in the "safe modeling zone" and our model should not

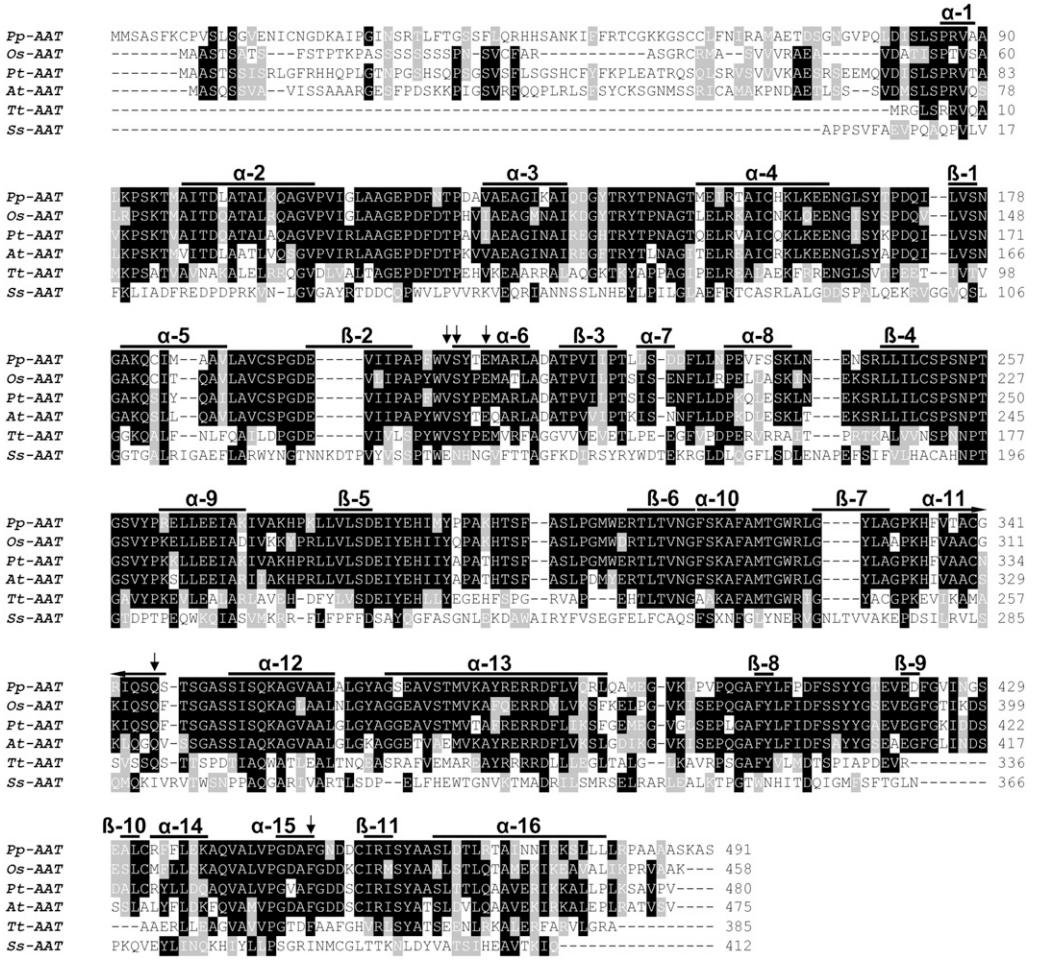

Figure 1. Protein sequence alignment of plant PT-AATs with bacterial and eukaryotic AAT models. Sequences were aligned with ClustalW followed by manual refinement using the hydrophobic cluster analysis method. Secondary structure motifs determined for the *P. pinaster* sequence (α-helices and β-strands) are indicated. Residues selected for site-directed mutagenesis and functional analysis are marked by arrows. Sequences corresponding to plant PT-AAT, including the chloroplast transit peptide, were aligned. Gaps in the alignment are shown with gray dashes. Identical residues are shown in black, and similar residues are shown in gray. PpAAT, *P. pinaster* PT-AAT; OsAAT, *O. sativa* PT-AAT; PtAAT, *P. trichocarpa* PT-AAT; AtAAT, *A. thaliana* PT-AAT; TtAAT, Iβ-type AAT from *T. thermophilus*; SsAAT, Iα-type AAT from *S. scrofa*.

have significant errors, assuming a standard alignment. Nevertheless, a manually created alignment was used for the initial modeling. The complete sequence for PpAAT was larger than that of the template ttAAT. Therefore, the plastid-targeting peptide plus 15 residues in the PpAAT N terminus and 10 residues in the C terminus were not included in the model. The region under analysis consisted of the amino acid residues from Asp-81 to Leu-478 in the PpAAT primary sequence. Along this polypeptide fragment, PpAAT and ttAAT are 42% identical. To achieve a reliable model of the quaternary structure for both the apoenzyme and PpAAT in the internal aldimine form, we relaxed the system via energy minimization and molecular dynamics simulations over 1 ns. Based on this, we have obtained the basic structure that will be used for further spectroscopic and mutagenesis studies.

There is no resolved structure for plant type Iβ AAT, and only one plant type Iα has been reported to date (Wilkie et al., 1996). Our model represents, to our knowledge, the first molecular model for a type Iβ AAT in eukaryotes. The modeled enzyme exists as a homodimer based on the experimental data previously described by de la Torre et al. (2006). The way the two subunits might fit together is illustrated in Figure 2. The dimer contains two equivalent active sites, each of which is formed by residues from both subunits. The overall folding of the PpAAT model resembles the known structures for other AATs belonging to both subfamily Iα and Iβ, such as *E. coli* (Okamoto et al., 1994), yeast (Jeffery et al., 1998), pig (Rhee et al., 1997), chicken (Malashkevich et al., 1995), *T. thermophilus* (Nakai et al., 1998), and *P. lapideum* (Kim et al., 2003).

Nearly all of the AAT enzymes that have been studied are composed of two identical monomers. Each monomer is folded and is composed of a large domain, a small domain, and an extended N-terminal arm, the end of which interacts with the other monomer. The domain division was first established for chicken mitochondrial AAT and for pig cytosolic AAT on the basis of the correlated motion of N-terminal and C-terminal parts of a polypeptide chain upon inhibitor binding (Malashkevich et al., 1995; Rhee et al., 1997). The AAT domain distribution described in these enzymes was later used to establish the ttAAT domain distribution (Nakai et al., 1999). According to the model developed in this work, each monomer of the PpAAT enzyme is equally composed of a small and a large domain (Fig. 2B). The domains in the PpAAT monomer were identified through comparison with the primary sequence of the closely related ttAAT polypeptide (Nakai et al., 1999). The small domain is formed by two parts of the polypeptide chains, spanning Lys-92 to Asn-124 and Met-376 to at least Leu-478. The large domain contains the residues between Asn-124 and Met-376. Residues 81 to 92, which are part of the N-terminal arm, are located at the surface of the large domain of the opposite monomer (Fig. 2B). The quaternary structure representation of PpAAT, based on the model described in this study, is fully in agreement with the previously described domain distribution as determined by comparison with the ttAAT amino acid sequence. These data support the accepted conclusion that all AAT enzymes, independent of whether they belong to subfamily Iα or Iβ, display a very similar 3D structure (Nakai et al., 1998, 1999). Comparison of the domain distribution in the prokaryotic and eukaryotic types of AAT (PpAAT, ttAAT, and SsAAT) clearly shows how these enzymes, which differ considerably in their primary structure, maintain highly similar tertiary and quaternary structures (Fig. 3). However, an asymmetric distribution of the hydrophobic amino acids His, Phe, Trp, and Tyr over the enzyme surface has been observed. This molecular feature was particularly evident in the large domain of the prokaryote-type enzyme but absent in the eukaryote-type AAT.

The secondary structure of PpAAT was compared with that of ttAAT, and a high level of correlation was found in the distribution of α-helix and β-strand motifs. Each PpAAT monomer is composed of 16 α-helices and 11 β-strands (Figs. 1 and 3). The core of the large domain is formed by a wide β-sheet structure, which is composed of six β-strands arranged parallel (p) and one arranged antiparallel (a), with the distribution pppppap. The seven β-strands have a tendency to twist right-handedly, which appears to be a β-sheet with a left-handed twist when viewed along the β-sheet normal to strands. This structure is highly conserved in other AAT enzymes, including the chlo-

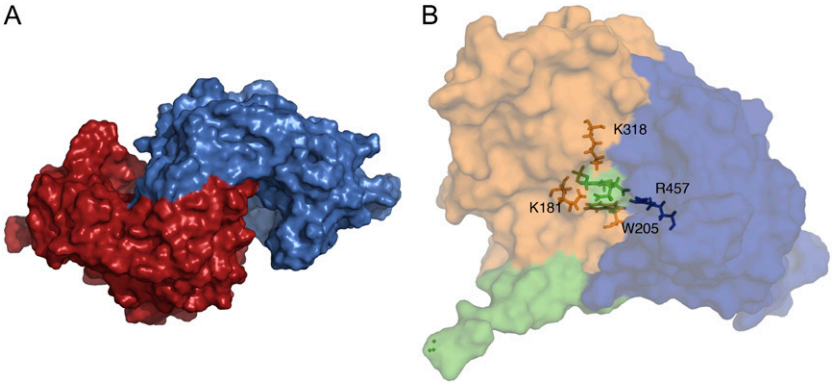

Figure 2. PpAAT tertiary and quaternary structures. A, Space-filling representation of PpAAT homodimer. Each color, red or blue, corresponds to a subunit. B, Space-filling representation of small (blue) and large (orange) domains in a single PpAAT monomer. The arm (green) between both domains corresponds to the N-terminal sequence of the modeled PpAAT that includes residues Ile-82 to Lys-92. The positions of the PLP cofactor and relevant residues in the center of the monomer are indicated.

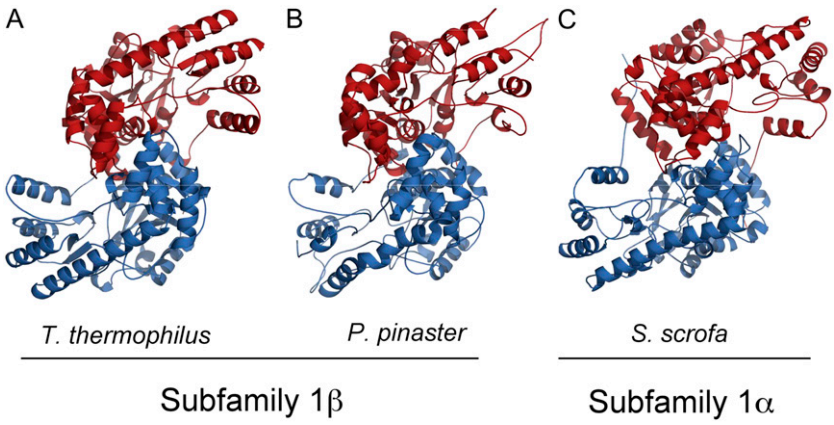

Figure 3. Comparison of the 3D structures of PpAAT (B) and the bacterial (*T. thermophilus*; A) and eukaryotic (*S. scrofa*; C) AAT models. Each color, red or blue, corresponds to a subunit of the dimeric enzyme.

roplastic isoform of Arabidopsis, which is a eukaryote-type AAT (Wilkie et al., 1996). The small domain is composed of four short β-strands and five α-helices. The β-strands are grouped pairwise in a parallel-antiparallel conformation and are arranged into two small β-sheet regions. As described in other subfamily Iβ AATs, a high Pro content was found when compared with the low content reported for mesophilic AATs. In addition, the thermolabile amino acids Cys and Asn are represented at a low level.

Structural Analysis of the PpAAT Active Center and Prediction of Residues Involved in the Recognition of Acidic Substrates

The structure of the active center of PpAAT was deduced using information derived from two sources. The first one comprises the prediction derived from both the model and the comparison with x-ray crystal structures corresponding to other subfamily Iβ members. The second source of information consists of experimental results describing the residues involved in the catalytic mechanism reported in AATs from different organisms, such as *E. coli* or pig (*S. scrofa*). The model developed for PpAAT follows the pattern previously described in plAAT and ttAAT, with conservation of the main features of the active-site region (Fig. 4). The essential residues Tyr-144, Trp-205, Tyr-287, Lys-318, and Arg-457 are quite well conserved. The PLP cofactor is virtually positioned within the predicted region in the active site attached to Lys-318, via a covalent imino linkage between C-4′ of the cofactor and the ε-amino group of the Lys residue. Lys-318 is the equivalent residue in PpAAT to the pig cytosolic enzyme's Lys-258 (Mehta et al., 1989). The relative positions of the other residues involved in the interaction with the cofactor were located (data not shown). These interactions, which are important for the correct positioning of the cofactor within the active site, seem to be satisfied by our model.

The stabilization of the acidic substrates, Glu and Asp, within the AAT enzyme is mainly carried out by the interaction of its carboxylic groups (α and γ) with specific residues in the active center. Arg-457 in PpAAT is conserved in the AATs from both the Iα and Iβ subfamilies. The side chain of this particular residue stabilizes the α-carboxylate group of the substrate in all known AAT enzymes. In addition, AAT enzymes of subfamily Iα have an Arg residue, which interacts with the distal carboxylate group of dicarboxylic (acidic) substrates and enhances the optimal catalytic positioning. This residue is characteristic of Iα AATs and is absent in the Iβ type, where a Lys residue has a similar role, as has been reported for the ttAAT enzyme (Nobe et al., 1998). This Lys residue (Lys-181 in the PpAAT model) is essential for the recognition of acidic substrates and is highly conserved in all Iβ AATs. However, it has been suggested that Lys-181 may require assistant residues for substrate recognition, since Arg is much more preferred for this purpose in many different enzymes (Nobe et al., 1998). Potential candidates for this role in the PpAAT active site are the conserved residues Val-206, Ser-207, and Gln-346 (Fig. 4).

Spectrophotometric Properties of the PpAAT Enzyme

Affinity-purified preparations of the PpAAT recombinant enzyme were spectrophotometrically characterized between 250 and 550 nm (Fig. 5). The enzyme showed a maximum in the absorption at 280 nm, which is due to the aromatic residue side chains, and another maximum at 385 nm, which is due to the bound cofactor. The PpAAT apoenzyme was separated from the PLP cofactor by incubation of the enzyme in the presence of phenylhydrazine (Fig. 5A). The spectral curve corresponding to the apoenzyme was determined between 250 and 550 nm, and a single maximum at 280 nm could be detected. When the spectral curve for PpAAT was determined in the presence of 10 mM Asp, the pyridoxamine-phosphate (PMP) form of the enzyme was detected as an absorption peak close to 329 nm (data not shown). This value is very close to the absorption peak at 327 nm observed for neutral aqueous PMP with a dipolar ionic ring and a protonated 4′-amino group (Kallen et al., 1985).

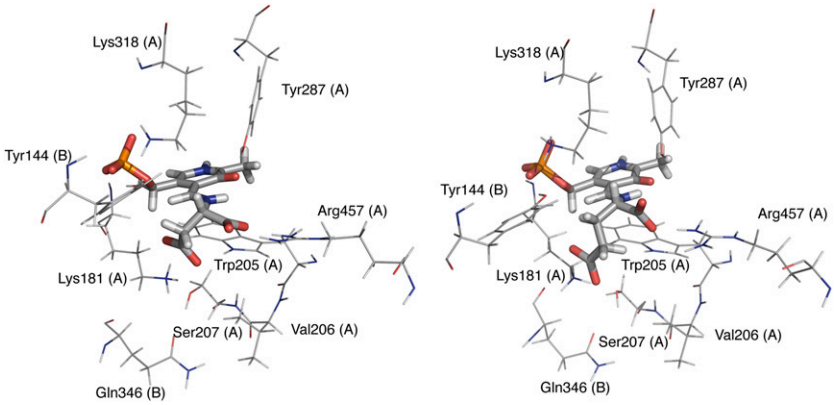

Figure 4. Structure of the active site of PpAAT. External aldimines are shown as sticks. The C4 substrate Asp is shown at left, and the C5 substrate Glu is shown at right. Relevant residues are depicted in wireframe representation. The contribution of each subunit to the active site is indicated as (A) or (B).

When the pH in the buffer containing the enzyme was reduced to acidic conditions, the enzyme showed an absorption band at 280 nm and the other maximum shifted to 425 nm. The enzyme showed higher activity when the pH was neutral or in slightly alkaline conditions, in which the band at 385 nm is the most prominent one (Fig. 5B). Similar spectral behavior related to pH changes has been extensively reported (Kim et al., 2003). These data suggest that the two forms are derived from the difference in the ionization state of the nitrogen atom of the internal Schiff base formed between the aldehyde group of PLP and the amino group of a lysyl residue of the enzyme (Braunstein, 1964). The isosbestic point was determined to be close to 406 nm, when considering the distinct spectral curves at different pH values.

Characterization of Residues Putatively Involved in the Interaction between PpAAT, Acidic Substrates, and PLP

In order to precisely determine the topology of interactions between the protein's active center, its substrates, and the cofactor PLP, we decided to introduce point mutations affecting key residues. Thus, three residues with putative roles as "assistants" in the stabilization of the substrate were selected in the PpAAT model. These were Val-206, Ser-207, and Gln-346. Val-206 is located between two residues involved in the stabilization of the substrate, but its hydrophobic side chain is predicted to be in the opposite direction. Ser-207 was selected because of its spatial position close to Lys-181, and it has an orientation that may putatively involve it in the stabilization of the distal carboxyl group of substrate and PLP. Gln-346, a residue that belongs to the other subunit in the dimer (Fig. 4), could also be involved in these interactions. In addition, these three residues are all conserved in Iβ-type enzymes and absent in Iα-type enzymes (Fig. 1). Site-directed mutagenesis was used to study the functional significance, if any, of these selected residues.

In our model, the hydrophobic side chain of Val-206 is immediately close to Trp-205, the amino acid residue that stabilizes the cofactor in conjunction with Tyr-287. In fact, the PLP pyridine ring is nearly parallel to the indole ring of Trp-205 (Fig. 4). The PpAAT Val-206 was replaced by a polar and hydrophilic Ser residue (V206S). The mutant protein was overexpressed and affinity purified (Fig. 6, A and B), and its activity was determined to be about 70% of that observed for the wild-type enzyme (Fig. 6C). A significant increase in the K_m values for the substrates of AAT in the forward reaction, with Asp and 2-oxoglutarate as substrates, was observed, whereas there was no change in the affinity of substrates for the reverse reaction, with Glu and oxaloacetate (Table I). Nevertheless, there was a considerable decrease in the absorbance of the cofactor

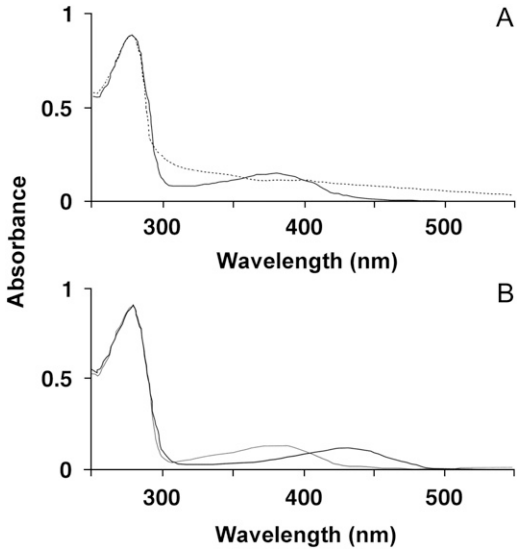

Figure 5. PpAAT is a PLP-dependent enzyme with variable absorption spectra depending on pH. A, PpAAT (solid line) absorption spectra between 250 and 550 nm compared with the absorption spectra of the same protein previously incubated in the presence of phenylhydrazine (dashed line). In both cases, protein solutions were purified and concentrated to 1 mg mL^{-1}. B, Absorption spectra of the PLP enzyme are represented at two different pH values. The solid black line corresponds to pH 5, and the solid gray line corresponds to pH 8. The buffers used were 0.1 M sodium acetate for pH 5 and Tris-HCl for pH 8. In both cases, the protein solutions were purified and concentrated to 1 mg mL^{-1}.

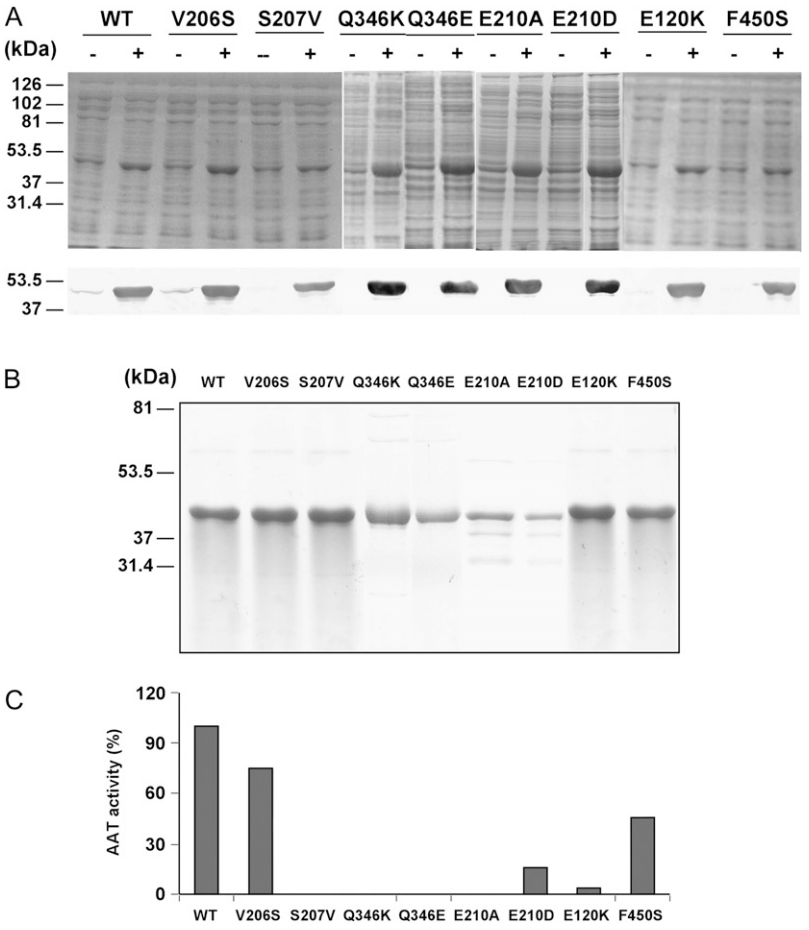

Figure 6. Recombinant production, purification, and functional analysis of the wild type and point mutants of the PpAAT enzyme. A, Bacterial cultures overexpressing PpAAT proteins in the BL21 DE3 PLys strain of *E. coli* were grown for 16 h at 10°C in the presence (+) or absence (−) of 1 mM isopropylthio-β-galactoside. Protein profiles of the soluble fractions are shown at top. At bottom, the presence of each mutant PpAAT protein in the soluble fraction corresponding to each culture was confirmed by western blot using specific antibodies (de la Torre et al., 2006). B, Aliquots of purified enzyme (0.2–2 μg) for the wild type and each PpAAT mutant were separated by SDS-PAGE and stained with Coomassie Brilliant Blue dye. C, AAT activity was measured in the same aliquots following the method described by Karmen et al. (1955) for the forward reaction. AAT activities are shown as relative values, with wild-type activity taken as 100% (5.6 nkat). AAT activity for the same samples was equally measured on gels following the method described by Wendel and Weeden (1989; data not shown). WT, Wild type.

when the absorption spectra corresponding to the V206S mutant was compared with the one corresponding to the wild-type enzyme (data not shown).

The oxygen of the Ser-207 hydroxyl is located close (2.6 Å) to the ε-amino group of Lys-181 in PpAAT. In other Iβ AAT enzymes, a similar distance, which was 2.7 Å in ttAAT and 3 Å in plAAT, was measured for the equivalent residues. Ser, which is a polar and hydrophilic residue, in position 207 was replaced by Val, which is an aliphatic and hydrophobic residue, with the goal of determining whether or not it has a role in the stabilization of the acidic substrate within the active center. Once the protein was overexpressed in *E. coli* and affinity purified (Fig. 6, A and B) with the His-tag technology, the enzyme activity was measured in both forward and reverse AAT reactions and in situ AAT activity was determined on native gels. No activity was detected in any of these assays for the S207V mutant enzyme (Fig. 6C). Furthermore spectrophotometric characterization of the S207V mutant protein showed that there was a transition of the characteristic absorption maximum at 383 to 331 nm, which is close to the absorption maximum observed for the PMP form of the enzyme (Supplemental Fig. 1).

According to the model, the Gln residue in position 346 forms hydrogen bonds with both Lys-181 and Ser-207 and, hence, may contribute to proper substrate positioning in the active center. Replacement of the Gln by either Lys or Glu could possibly affect the catalysis. After site-directed mutagenesis and the corresponding purification of the two mutant proteins (Q346K and Q346E), no enzyme activity was detected in the enzyme preparations (Fig. 5).

Characterization of Residues Putatively Involved in the Relative Domain Movement from "Small to Large" in PpAAT

Additional single-mutant proteins were designed in order to study in depth the reported mechanism by

Table I. *Substrate affinities (K_m) of wild-type and mutant PpAAT enzymes*

Kinetic parameters were not determined for enzyme mutants S207V, Q346K, Q346E, E210A, and E210K, which exhibited extremely low levels of AAT activity. All given values are in mM.

Enzyme	L-Asp	2-Oxoglutarate	L-Glu	Oxaloacetate
Wild type	2.50	0.08	1.0	0.18
V206S	14.00	0.60	1.0	0.20
E210D	5.3	0.20	1.3	0.55
F450S	2.50	0.09	1.0	0.19

which the small domain turns toward the large domain in the presence of the substrate. Glu-210 was replaced by Ala, Asp, or Lys through site-directed mutagenesis to generate the E210A, E210D, or E210K mutant. In the wild-type enzyme, Glu-210 seems to be linked through an electrostatic interaction with the Lys-92 residue in the pocket determined by surfaces corresponding to both the small and large domains (Supplemental Fig. 2). The enzyme variants E210A, E210D, and E210K were overexpressed, affinity purified, and functionally characterized (Fig. 6). The products of E210A and E210K mutants were almost inactive (Fig. 6C), and since the recovered activity was very low, no kinetic parameters could be determined (Table I). In contrast, the E210D mutant retained about 10% of the activity exhibited by the wild type (Fig. 6C). When the K_m values for the substrates were determined, a slight decrease in the affinity for substrates was observed in both the forward (Asp and 2-oxoglutarate) and the reverse (Glu and oxaloacetate) reactions (Table I). All of these results support the relevance of the acidic lateral side chain of Glu-210 for enzyme function.

Phe-450 is a residue common to all subfamily Iβ s and is not present in subfamily Iα enzymes. This hydrophobic residue is located in the same pocket described previously between the large and small domains. This pocket is a "hydrophobic-rich" region in the protein, with an internal structure that varies between the open and closed forms. The existence of a "hydrophobic patch" has been proposed in the case of *E. coli* AAT as part of a mechanism involved in the "driving forces" needed to complete the transition from the Michaelis complex to the external aldimine in the reverse reaction (Jäger et al., 1994; Okamoto et al., 1994; Islam et al., 2005). Using site-directed mutagenesis, Phe-450 was replaced by Ser (F450S), a hydrophilic residue, in order to determine its possible role in the catalytic mechanism. This residue is located on the internal surface of the small domain in a location close to a "hydrophilic region" that corresponds to the large domain and is composed of the residues Trp-205, Phe-204, and Tyr-208. When the activity was measured, a 50% decrease was observed with respect to the wild type. The K_m values for substrates in both the forward and reverse reactions were also measured, and no significant variation was detected when compared with the wild-type enzyme. This finding suggested that this residue could be involved in the progress of the enzymatic reaction rather than in substrate reception (Table I).

DISCUSSION

Structural Aspects of PpAAT

In this paper, the structure of maritime pine (*P. pinaster*) PT-AAT has been investigated in order to gain further insights into the function of this enzyme in plants. The computer modeling of the mature enzyme (PpAAT) was compared with the previously reported Protein Data Bank files of animal and bacterial AATs. A high level of similarity was observed in the spatial architecture of the enzyme, even when different levels were considered (Kallen et al., 1985; McPhalen et al., 1992; Jäger et al., 1994; Okamoto et al., 1994). The overall secondary structure described for PpAAT is highly conserved throughout all AAT enzymes. Some of the conserved key elements include the seven β-strand-β-sheet that constitutes the core of the large domain, the N-terminal flexible α-helix, and the distribution of α-helices throughout the enzyme. The monomer is also organized into a large and a small domain that flanks the active site pocket, as reported for the tertiary structure of other AAT enzymes. When the quaternary structure of PpAAT is analyzed, the docking of two identical monomers into a homodimeric enzyme is in agreement with the other AATs and with our previous results (de la Torre et al., 2006). Despite the high structural similarities, the identities between their amino acid sequences are low. These results suggest that the AAT spatial structures are highly limited by their "catalytic needs" and that only minor 3D variations are allowed.

Multiple alignments, which have been built from AATs of distant species, clearly show that most of the residues involved in the well-known catalytic mechanism described for the subfamily Iα (Okamoto et al., 1994; Rhee et al., 1997) are conserved in PpAAT. When the active center in the PpAAT structure is compared with those from prokaryotic enzymes (*T. thermophilus* and *P. lapideum*), a nearly total identity is found. Similar characteristics are also found when PpAAT is compared with AATs from subfamily Iβ for other features, such as Pro content (Kim et al., 2003), substrate specificity (Ura et al., 2001), and thermostability (Nobe et al., 1998). Taken together, these data suggest that the plant enzyme has retained the structural and functional properties of the prokaryotic AATs.

Previous data showed that PpAAT is a highly stable enzyme under a wide range of temperatures up to 75°C (de la Torre et al., 2007). Its thermostability seems to be related to its amino acid composition with a high Pro content (6.4%), which results in an enzyme with a rigid and packed structure. The *T. thermophilus* AAT has also been reported to be a thermostable, rigid enzyme with the exception of the N-terminal α-helix (H1), which is composed of amino acid residues 16 to 28. An identical helix with an equivalent position and orientation is present in the PpAAT enzyme and is composed of residues 96 to 109. In both enzymes, this H1 α-helix is connected to the next α-helix (H2) by an almost completely conserved region. This linking region is composed mainly of small amino acids (AGEPDFNTP) and is common to all subfamily Iβ AATs that have the H1 motif. The binding of the inhibitor maleate to ttAAT induces a conformational change from the open to the closed form, and this has also been reported for AAT subfamily Iα enzymes

(Nakai et al., 1999). This change does not affect the whole small domain, as only the N-terminal region that is mainly composed of the α-helix H1 approaches in order to close the active site (Nakai et al., 1999). The highly conserved region linking H1 and H2 is composed of small amino acids that allow an efficient rotation due to the low rotation restriction around ψ and ϕ angles. This region could be involved in the "open-to-closed" movement of the domains. Futures studies with substitution by site-directed mutagenesis will help to determine the role of this region on the catalytic mechanism.

A significant structural difference between members of subfamily Iβ is the presence of 10 to 11 amino acid residues in the plant PT-AATs, corresponding to positions 421 to 432 in the PpAAT sequence that are absent in bacterial AATs. This particular region was depicted in the model as a short helix that is located outside the active center (Supplemental Fig. 3). Whether or not this structural feature has a potential role in the plant PT-AATs will require further studies.

Substrate Recognition in the PpAAT Enzyme

Dicarboxylate substrates are recognized, stabilized, and correctly oriented into the AAT active center through the interactions of their α- and γ-carboxyl groups with the side chains of residues that are located within the "catalytic pocket." The α-carboxyl group in the substrate is recognized and stabilized by an Arg residue in all AATs that have been described to date. The interaction between the distal (γ) carboxyl group and the enzyme is carried out in subfamily Iα AATs through an Arg residue. Based on previous work that described the recognition of the distal carboxyl group of acidic substrates into the *T. thermophilus* active center, it has been proposed that this role is mainly carried out by a Lys residue that is exclusively found in subfamily Iβ AATs (Nobe et al., 1998). The equivalent residue has been determined to be Lys-181 in PpAAT. This residue has been designated as a major determinant of the acidic substrate specificity.

The "Ra" type has been described as the mode of interaction between an Arg side chain and a substrate's carboxylic groups. This type of interaction describes the recognition of α-carboxylic groups in all AATs and the interaction with the distal carboxylic groups in subfamily Iα. This interaction does not need additional residues for correct charge compensation and it thought to be the most frequent type of interaction in enzymes that use carboxylic substrates. In contrast, the recognition of a carboxyl group through a Lys residue has been described as extremely rare. It has been proposed that assistant residues would be required to stabilize substrates in that case (Islam et al., 2005). Site-directed mutagenesis showed that the introduction of Arg-292 into the *T. thermophilus* AAT is a key step in the change of only the acidic substrate specificity in an enzyme that has dual acidic and hydrophobic substrate specificity (Ura et al., 2001).

We modeled the external aldimines for the C4 and C5 dicarboxylic substrates in the closed conformation, since it seems that the reaction proceeds when the enzyme is in its closed form. It is clear that the binding of the C4 substrate induces a conformational change in the enzyme from the open to the closed form, and it was recently reported that, for the C5 substrate, this conformational transition occurs from the open form in the Michaelis complex to the closed form in the external aldimine (Islam et al., 2005). Since our main objective was to increase our knowledge about the acidic substrate specificity of PpAAT, the vicinity of Lys-181 was analyzed in order to identify other amino acid residues in the active center that could be implicated in substrate stabilization. The existence of a hydrophobic cavity around the Lys-181 area was revealed. The cavity is composed of the residues Phe-450, Phe-204, Tyr-144 (opposite chain), Tyr-208, Tyr-329, Val-313, Val-188, Val-206, and Trp-205.

The Val-206 residue is located very close to Trp-205. Based on the structure described for ttAAT, the equivalent residue of Trp-205 has been proposed to be involved in the stabilization of the PLP pyridine ring by its side chain (Nakai et al., 1999). In *E. coli* AAT, the N(1) of the equivalent residue of Trp-205 seems to be partly involved in the binding of the distal carboxylate group of the dicarboxylic substrates (Hayashi et al., 1990). In PpAAT, however, we observed that this interaction mainly occurs with C4 dicarboxylic substrates (Fig. 4). The distances between the nitrogen atom from the indole group and the γ-carboxylic group are 2.9 Å for the C4 substrate and 4.1 Å for the C5 substrate.

When Val-206 was changed to Ser, a significant decrease in the activity was observed (about 30%). The kinetic parameters for the reverse reaction were not altered, while the K_m values for substrates in the forward reaction (Asp and 2-oxoglutarate) were increased by 1 order of magnitude. The hydrophobic-to-hydrophilic (V206S) substitution seems to alter the correct orientation of the aromatic side chain of Trp-205, which should face the pyridine ring of PLP. This substitution likely altered the correct orientation of PLP within the active center and, thus, affected the affinity for the substrates in the forward reaction. If so, the active center has been altered in a way that does not affect the reverse reaction. Considering the data reported by Islam et al. (2005), the catalytic transition changes are not equivalent in both the forward and reverse reactions. The binding of Glu to AATs to form the Michaelis complex does not induce a conformational change in the enzyme in an opposite way, as described for the formation of the Michaelis complex with Asp. Our data suggest that the altered PLP orientation proposed for the V206S mutant is more critical for the conformation of the Michaelis complex in the closed form than the Michaelis complex conformation in the open form, which is needed for the reverse reaction. Another possible explanation for the asymmetric alteration of kinetic parameters can be

related to the indirect alteration of the orientation of Lys-181 through the movement of Trp-205 that occurs as a result of the V206S change. This option suggests that the orientation of Lys-181 could be influenced by the hydrophobic pair Val-206/Trp-205 in the closed (Asp) form but not in the open (Glu) form.

The Ser-207 and Gln-346 residues were also selected as candidates to be analyzed, since they are unique residues that are close to Lys-181 within the active site. Ser-207 is from the same subunit and Gln-346 is from the other one. Based on our PpAAT model, the distance between the Ser-207 hydroxyl oxygen and the σ-amino nitrogen is 2.7 Å for the C4 substrate and 2.9 Å for the C5 substrate. Gln-346 directly interacts with Ser-207 and, therefore, may contribute to substrate stabilization. In order to study the importance of these two residues in the stabilization of Lys-181 in the correct orientation, Ser-207 was replaced by a Val, whereas Gln-346 was changed to either a basic (Lys) or an acidic (Glu) residue. The replacement of Ser-207 by the hydrophobic Val residue yielded a mutant protein that lacked the target bond that appears to be critical in the stabilization of Lys-181. Similarly, the ability to establish hydrogen bonds at position 346 is lacking in the Q346K and Q346E mutants. The activity of the S207V, Q346K, and Q346E enzymes was completely abolished in both forward and reverse AAT reactions (Fig. 6). These data indicate that Ser-207 and Gln-346 are essential assistant residues involved in the correct positioning of Lys-181 and, therefore, involved in substrate recognition.

The negatively charged residue Glu-210 was also selected for functional analysis, again using site-directed mutagenesis. The model structure predicts that the negatively charged Glu-210 residue can electrostatically interact with the positive charge of a Lys-92 residue. These two residues, Glu-210 and Lys-92, are located in the large and small domains, respectively. Lys-92 is specifically positioned in the small domain, just beside the α-helix (H1) at residues 96 to 109. Therefore, it is deeply involved in the open-to-closed conformational change, given that it is positioned in the H6 α-helix of the large domain. The mutant proteins E210A and E210K showed a dramatic decrease of AAT activity in relation to the wild-type enzyme, which suggested that the acidic lateral side chain of Glu-210 is required for enzyme activity. The replacement of Glu by Asp further supports the above assumption. Thus, the E210D mutant enzyme was partially active, although its activity was much lower than in the wild type, and it exhibited decreased affinity for its substrates. Taken together, these data suggest that alteration in the electrostatic interaction between Lys-92 and Glu-210 affects the ability of the

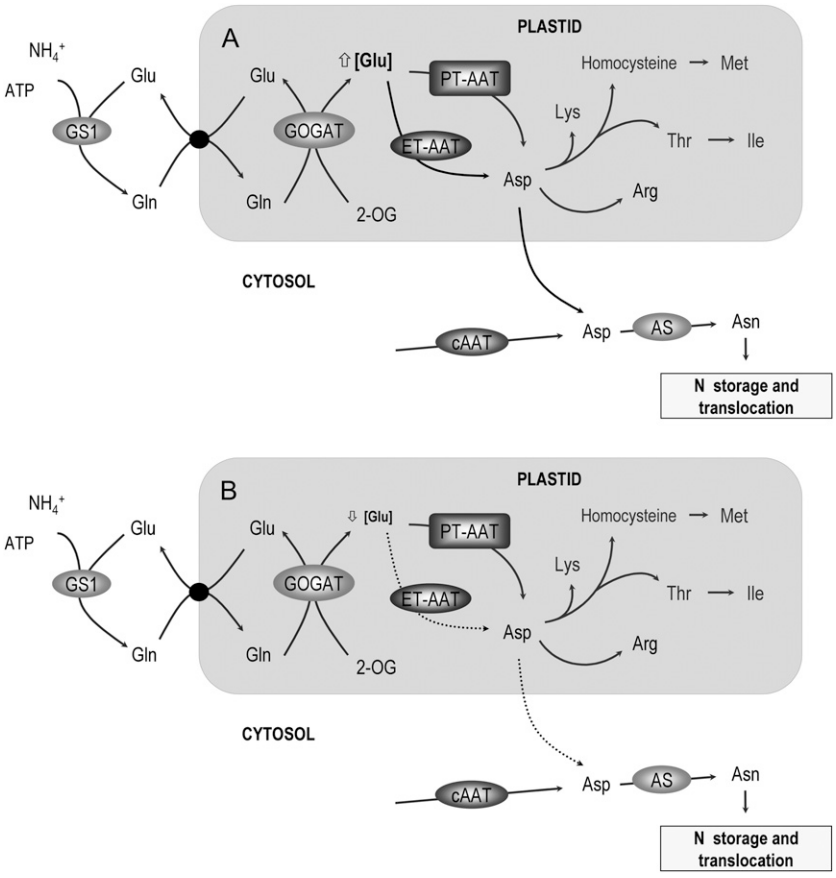

Figure 7. Putative models for the role of plastidic AATs. A, High Glu abundance. B, Low Glu abundance. AS, Asn synthetase; cAAT, cytosolic AAT; ET-AAT, eukaryote-type AAT; GS1, cytosolic Gln synthetase.

enzyme to correctly develop the open-to-closed catalytic step. Further functional studies of the residues in the H1 α-helix will be needed to gain a better understanding about this critical mechanism that is characteristic of the subfamily Iβ AATs.

Data derived from the characterization of the F450S mutant suggests that this well-conserved residue has a relevant but not critical role in the enzyme. The reduced activity of the F450S mutant enzyme and the 3D location of Phe-450 indicates that this hydrophobic residue seems to be a member of a hydrophobic patch that is located within the pocket formed between the large and small AAT domains. The existence of these hydrophobic patches has been reported previously in AAT enzymes (McPhalen et al., 1992, Jäger et al., 1994).

Importance of Structural Studies to Understand the Metabolic Function of PT-AAT and Biotechnological Applications

The presence of Lys-181, a residue with a shorter side chain than Arg, in the catalytic site of PpAAT possibly favors optimal interactions with the substrate Glu. This could explain why Lys rather than Arg is conserved at this particular position in the subfamily Iβ AATs. We propose that Ser-207 and Gln-346 may function as assistants to fix the orientation of the distal carboxyl groups of the substrates. The structure of a more flexible catalytic site in the subfamily Iβ AAT enzymes could facilitate the recognition of Glu. These structural features are consistent with the kinetic behavior of the enzyme. Thus, the kinetic properties of PpAAT for Asp and 2-oxoglutarate are quite similar to those reported for the eukaryote-type AAT in plants. The affinity of PpAAT for Glu (K_m = 1 mM; de la Torre et al., 2006), however, is much higher than that reported for plastidic and other eukaryotic AATs, where the K_m values range between 10 and 30 mM (Taniguchi et al., 1995; Wilkie and Warren, 1998). Under conditions of steady-state photosynthesis, the concentration of Glu in the chloroplast ranges between 15 and 50 mM (Riens et al., 1991; Winter et al., 1994), which is well above the K_m value of PpAAT for this substrate. In contrast, the concentration of 2-oxoglutarate has been estimated to be in the micromolar range and even lower in the chloroplast stroma, because the Gln synthetase/GOGAT cycle represents a strong sink (Weber and Flügge, 2002). Consequently, a high Glu/2-oxoglutarate ratio in the stroma would drive biosynthetic transaminations that favor Asp biosynthesis. Under these conditions, the eukaryotic and prokaryotic forms of plastidic AAT would be saturated and the flux toward Asp biosynthesis would be very high through the catalytic action of both enzymes (Fig. 7A). However, under physiological conditions in which Glu abundance is low (e.g. limited nitrogen availability and other stressful conditions), only the PT-AAT isoenzyme would ensure the biosynthesis of Asp-derived amino acids and other nitrogen compounds in the plastids (Fig. 7B). A main pathway of Asp utilization is the biosynthesis of the Asp-derived amino acids Lys, Thr, Ile, and Met, all of which are required for protein synthesis and produced exclusively in the plastid (Azevedo et al., 2006). All of these amino acids are essential in the nutrition of animals, in which PT-AAT does not exist (de la Torre et al., 2006).

In cyanobacteria, inorganic nitrogen is assimilated through the Gln synthetase/GOGAT cycle and turned into Glu, which is then utilized as an amino donor by AAT and other transaminases for the biosynthesis of nitrogen compounds (Muro-Pastor et al., 2005). PT-AAT could play a similar role in the chloroplasts of higher plants that utilize Glu for amino acid biosynthesis inside that organelle (Cánovas et al., 2007). The results reported here suggest that the structure of the catalytic site is adapted for the optimal utilization of Glu for the biosynthesis of nitrogenous compounds. Molecular and physiological analysis of overexpressing and knockout lines of transgenic plants will be required to determine the role of the enzyme in plant nitrogen metabolism. Pagnussat et al. (2005) reported the identification of 130 transposon mutants of Arabidopsis that have defects in female gametogenesis and embryo development. One of these lines, a mutant defective in the At2g22250 locus, was affected in early embryo development, which indicates a potential role for PT-AAT in nitrogen metabolism during embryogenesis.

MATERIALS AND METHODS

Computer Modeling of the Spatial Structure of PpAAT

A homology model of *Pinus pinaster* AAT (residues 81–478) was built using crystal structures of AAT from *Thermus thermophilus* as a template in both open and closed conformations (Protein Data Bank accession nos. 1BJW and 1BKG, respectively). The PpAAT sequence was isolated from a *P. pinaster* EST database of different woody tissues in a previous work (de la Torre et al., 2006). Alignments were performed with ClustalW (Thompson et al., 1994) and manually edited. The whole PpAAT polypeptide fragment was modeled with modeller 9v1 (Sali and Blundell, 1993) on a GNU/Linux box. Structure quality and minor structural conflicts were evaluated using the Discrete Optimized Protein Energy statistical potential within modeller (Shen and Sali, 2006). The quaternary structure of the enzyme was built through comparison with that of ttAAT following the steps described previously for other PLP-dependent enzymes (Rodríguez-Caso et al., 2003; Moya-García et al., 2005, 2008). External aldimine was also modeled for both the C4 substrate Asp and the C5 substrate Glu with PyMOL (DeLano, 2002a, 2002b). Using the structures of malic acid and PMP as a scaffold, we built the PLP-Glu and PLP-Asp external aldimines that were placed in the PpAAT active site by manual fitting and comparison with the positions of PMP and malic acid in the active site of ttAAT x-ray crystal structure. We built three different enzymatic systems: PpAAT in closed conformation with PLP-Asp, PpAAT in closed conformation with PLP-Glu, and PpAAT in open conformation (free enzyme). All of them were energy minimized and equilibrated using Langevin-Verlet molecular dynamics simulations (NVT ensemble) over 1 ns at a temperature of 298 K. The FORTRAN library DYNAMO (Field, 1999) and the OPLS force field were used to perform every simulation.

Site-Directed Mutagenesis via PCR

The PpAAT sequence used in this study was previously inserted in the *Nde*I-*Bam*HI cloning site of pET-11a vector (de la Torre et al., 2006). Single mutations were introduced into the cloned PpAAT using the QuickChange site-directed mutagenesis kit (Stratagene). Reactions were carried out using the following primer pairs: for V206S, 5′-CCAGCTCCATTTTG-

GTCAAGCTATACTGAAATGGCTCGG-3′ (sense) and 5′-CCGAGCCATTTCAGTATAGCTTGACCAAAATGGAGCTGG-3′ (antisense); for S207V, 5′-CCAGCTCCATTTTGGGTAGTCTATACTGAAATGGCTCGG-3′ (sense) and 5′-CCGAGCCATTTCAGTATAGCATACCCAAAATGGAGCTGG-3′ (antisense); for E210K, 5′-CCATTTTGGGTAAGCTATACTAAAATGGCTCGGTTAGC-3′ (sense) and 5′-GCTAACCGAGCCATTTTAGTATAGCTTACCCAAAATGG-3′ (antisense); for E210A, 5′-GGTAAGCTATACTGCAATGGCTCGGTTAGCAGATG-3′ (sense) and 5′-CATCTGCTAACCGAGCCATTGCAGTATAGCTTACC-3′ (antisense); for E210D, 5′-GGTAAGCTATACTGATATGGCTCGGTTAGCAGATG-3′ (sense) and 5′-CATCTGCTAACCGAGCCATATCAGTATAGCTTACC-3′ (antisense); for F450S, 5′-GTCCCAGGAGATGCCTCCGGCAATGATGACTGC-3′ (sense) and 5′-GCAGTCATCATTGCCGGAGGCATCTCCTGGGAC-3′ (antisense); for Q346K, 5′-GTGGAAGAATTCAGAGCAAGTCCACATCAGGTGC-3′ (sense) and 5′-GCACCTGATGTGGACTTGCTCTGAATTCTTCCAC-3′ (antisense); and for Q346E, 5′-GTGGAAGAATTCAGAGCGAGTCCACATCAGGTGC-3′ (sense) and 5′-GCACCTGATGTGGACTCGCTCTGAATTCTTCCAC-3′ (antisense). The presence of the introduced mutations in the cDNA was confirmed by DNA sequencing.

Expression and Purification of Recombinant Wild-Type and Mutant Versions of PpAAT Enzymes

The optimal level of soluble recombinant PpAAT was previously reported to be obtained with the following procedure. Briefly, the cDNA-coding region for mature PpAAT was subcloned into the pET11a vector that included an N-terminal 6×His tag. Plasmid constructions were transformed in the *Escherichia coli* strain BL21-codonPlus-(DE3)-RIL (Stratagene). Transformed cells were grown at 37°C, with shaking in Luria-Bertani broth containing 100 μg mL^{-1} ampicillin and 34 μg mL^{-1} chloramphenicol, until a cell density (optical density at 600 nm) of 0.6 to 0.8 was reached. Flasks containing the cultures were supplemented with isopropyl-β-D-thiogalactopyranoside at a final concentration of 1 mM. Cells were then cultured at 10°C for 14 h with vigorous shaking. Cells were collected, and pellets were resuspended in a buffer containing 50 mM Na_2HPO_4, 300 mM NaCl, and 10 mM imidazole buffer at pH 8. Cells were lysed by sonication, and cell debris was removed by centrifugation at 22,000*g*. Recombinant proteins were purified by affinity chromatography using a nickel-nitrilotriacetic acid agarose column (Qiagen) under native conditions. An identical procedure was successfully used to overexpress and purify the PpAAT mutant versions V206S, S207V, Q346K, Q346E, E210A, E210D, E210K, and F450S.

Determination of Enzyme Activities

AAT activity was determined for both forward and reverse reactions. Direct reaction was determined by coupling the production of oxaloacetate from Asp and 2-oxoglutarate to the oxidation of NADH with malate dehydrogenase (Yagi et al., 1985). Reactions were developed in a mix solution containing 50 mM Tris-HCl, pH 7.8, 50 mM Asp, 10 mM 2-oxoglutarate, 0.07 mM PLP, 0.1 mM NADH, 2 units of malate dehydrogenase (Roche Farma), and the appropriate amount of enzyme in a final volume of 700 μL. The reaction was started by the addition of 2-oxoglutarate. The decrease in the levels of NADH was measured at 340 nm for a period of 120 s. The reverse reaction was measured by coupling AAT activity to the reaction catalyzed by Glu dehydrogenase in a mixture containing 15 mM Glu, 1 mM oxaloacetate, 0.1 mM NADH, 5 units of beef Glu dehydrogenase (Roche), 0.07 mM PLP, and 3.1 mM NH_4Cl in 60 mM potassium phosphate buffer, pH 7.5, at a final volume of 1 mL. The reaction was initiated by the addition of Glu and followed by the decrease of NADH at 340 nm for a period of 120 s.

AAT Activity on Native Gels

AAT recombinant enzymes were electrophoresed under nondenaturing conditions through a discontinuous, nondenaturing polyacrylamide gel with a 5% polyacrylamide stacking gel (37.5:1 acrylamide:bisacrylamide, 125 mM Tris-HCl, pH 6.8) and an 8% separating gel (37.5:1 acrylamide:bisacrylamide, 375 mM Tris-HCl, pH 8.8). The running buffer was 25 mM Tris-HCl and 250 mM Gly, pH 8.3. The gels were run at 15 mA for 90 min at 4°C. They were then placed in a bath containing 50 mL of AAT substrate solution with low shaking for 5 min. AAT activity was detected when the AAT substrate solution was supplemented with 1 mg mL^{-1} Fast Blue (Sigma). The composition of the AAT substrate solution (pH 7.4) was 2.2 mM 2-oxoglutarate, 8.6 mM Asp, 0.5% (w/v) polyvinylpyrrolidone-40, 1.7 mM EDTA, and 100 mM Na_2HPO_4 (Wendel and Weeden, 1989).

Protein Electrophoresis and Western-Blot Analysis

Proteins were separated by gel electrophoresis under denaturing conditions as described elsewhere (Cánovas et al., 1991). Both electroblotting from SDS gels to nitrocellulose membranes and immunodetection of AAT polypeptides were carried out as described elsewhere (de la Torre et al., 2002).

Phenylhydrazine Treatment

Pure PpAAT enzyme preparations were incubated at 50 mM phenylhydrazine (pH 7.4) at 37°C for 1 h, followed by gel filtration on a Sephadex G-25 column equilibrated with 50 mM potassium phosphate buffer, pH 7.4. Both phenylhydrazine-treated and untreated protein samples were characterized by spectrophotometric absorption between 250 and 550 nm.

Supplemental Data

The following materials are available in the online version of this article.

Supplemental Figure S1. Comparison of the absorption spectra of the PpAAT wild-type and S207V enzymes.

Supplemental Figure S2. Detailed view of the interaction between the large and small domains in the PpAAT structure.

Supplemental Figure S3. Location in the PpAAT structure of the short sequence stretch (10–11 amino acid residues) that is absent in bacterial enzymes.

ACKNOWLEDGMENTS

We are grateful to Dr. S. Martí from the Universitat Jaume I and to Dr. J. Ruiz-Pernía from the Universitat de València for their valuable advice. We also thank the Unidad de Efectos del Medio from the Universitat de València for computational support.

Received December 17, 2008; accepted January 23, 2009; published January 28, 2009.

LITERATURE CITED

Azevedo RA, Lancien M, Lea PJ (2006) The aspartic acid metabolic pathway, an exciting and essential pathway in plants. Amino Acids **30:** 143–162

Braunstein AE (1964) Binding and reactions of the vitamin-B6 coenzyme in the catalytic center of aspartate aminotransferase. Vitam Horm **22:** 451–484

Cánovas FM, Avila C, Cantón FR, Cañas RA, de la Torre F (2007) Ammonium assimilation and amino acid metabolism in conifers. J Exp Bot **58:** 2307–2318

Cánovas FM, Cantón FR, Gallardo F, García-Gutiérrez A, de Vicente A (1991) Accumulation of glutamine synthetase during early development of maritime pine (*Pinus pinaster*) seedlings. Planta **185:** 372–378

DeLano WL (2002a) The PyMOL Molecular Graphics System. DeLano Scientific, San Carlos, CA

DeLano WL (2002b) Unraveling hot spots in binding interfaces: progress and challenges. Curr Opin Struct Biol **12:** 14–20

de la Torre F, De Santis L, Suárez MF, Crespillo R, Cánovas FM (2006) Identification and functional analysis of a prokaryotic-type aspartate aminotransferase: implications for plant amino acid metabolism. Plant J **46:** 414–425

de la Torre F, García-Gutiérrez A, Crespillo C, Cantón FR, Avila C, Cánovas FM (2002) Functional expression of two pine glutamine synthetase genes in bacteria reveals that they encode cytosolic isoenzymes with different molecular and catalytic properties. Plant Cell Physiol **43:** 802–809

de la Torre F, Suárez MF, Santis L, Cánovas FM (2007) The aspartate am-

inotransferase family in conifers: biochemical analysis of a prokaryotic-type enzyme from maritime pine. Tree Physiol **27:** 1283–1291

Field MJ (1999) A Practical Introduction to the Simulation of Molecular Systems. Cambridge University Press, New York

Gantt JS, Larson RJ, Farnham MW, Pathirana SM, Miller SS, Vance CP (1992) Aspartate aminotransferase in effective and ineffective alfalfa nodules: cloning of a cDNA and determination of enzyme activity, protein, and mRNA levels. Plant Physiol **98:** 868–878

Jeffery CJ, Barry T, Doonan S, Petsko GA, Ringe D (1998) Crystal structure of *Saccharomyces cerevisiae* cytosolic aspartate aminotransferase. Protein Sci **7:** 1380–1387

Hayashi H, Inoue Y, Kuramitsu S, Morino Y, Kagamiyama H (1990) Effects of replacement of tryptophan-140 by phenylalanine or glycine on the function of *Escherichia coli* aspartate aminotransferase. Biochem Biophys Res Commun **167:** 407–412

Islam MM, Goto M, Miyahara I, Ikushiro H, Hirotsu K, Hayashi H (2005) Binding of C5-dicarboxylic substrate to aspartate aminotransferase: implications for the conformational change at the transaldimination step. Biochemistry **44:** 8218–8229

Jäger J, Moser M, Sauder U, Jansonius JN (1994) Crystal structures of *Escherichia coli* aspartate aminotransferase in two conformations: comparison of an unliganded open and two liganded closed forms. J Mol Biol **239:** 285–305

Jensen RA, Gu W (1996) Evolutionary recruitment of biochemically specialized subdivisions of family I within the protein superfamily of aminotransferases. J Bacteriol **178:** 2161–2171

Kallen RG, Korpela T, Martell AE, Matsushima Y, Metzler CM, Metzler DE, Morozov YV, Ralston IM, Savin FA, Torchinsky YM, et al (1985) Chemical and spectroscopic properties of pyridoxal and pyridoxaramine phosphates. *In* P Christen, DE Metzler, eds, Transaminases. John Wiley & Sons, New York, pp 215–234

Karmen A, Wroblewski F, Ladue JS (1955) Transaminase activity in human blood. J Clin Invest **34:** 126–131

Kim H, Ikegami K, Nakaoka M, Yagi M, Shibata H, Sawa Y (2003) Characterization of aspartate aminotransferase from the cyanobacterium *Phormidium lapideum*. Biosci Biotechnol Biochem **67:** 490–498

Madhusudhan MS, Marti-Renom MA, Eswar N, John B, Pieper U, Karchin R, Shen MY, Sali A (2005) Comparative protein structure modeling. *In* JM Walker, ed, The Proteomics Protocols Handbook. Humana Press, New York, pp 831–860

Malashkevich VN, Strokopytov BV, Borisov VV, Dauter Z, Wilson KS, Torchinsky YM (1995) Crystal structure of the closed form of chicken cytosolic aspartate aminotransferase at 1.9 A resolution. J Mol Biol **247:** 111–124

McPhalen CA, Vincent MG, Picot D, Jansonius JN, Lesk AM, Chothia C (1992) Domain closure in mitochondrial aspartate aminotransferase. J Mol Biol **227:** 197–213

Mehta PK, Hale TI, Christen P (1989) Evolutionary relationships among aminotransferases: tyrosine aminotransferase, histidinol-phosphate aminotransferase, and aspartate aminotransferase are homologous proteins. Eur J Biochem **186:** 249–253

Moya-García AA, Medina MA, Sánchez-Jiménez F (2005) Mammalian histidine decarboxylase: from structure to function. Bioessays **27:** 57–63

Moya-García AA, Ruiz-Pernía J, Martí S, Sánchez-Jiménez F, Tuñón I (2008) Analysis of the decarboxylation step in mammalian histidine decarboxylase: a computational study. J Biol Chem **283:** 12393–12401

Muro-Pastor MI, Reyes JC, Florencio FJ (2005) Ammonium assimilation in cyanobacteria. Photosynth Res **83:** 135–150

Nakai T, Okada K, Akutsu S, Miyahara I, Kawaguchi S, Kato R, Kuramitsu S, Hirotsu K (1999) Structure of *Thermus thermophilus* HB8 aspartate aminotransferase and its complex with maleate. Biochemistry **38:** 2413–2424

Nakai T, Okada K, Kawaguchi S, Kato R, Kuramitsu S, Hirotsu K (1998) Crystallization and preliminary x-ray characterization of aspartate aminotransferase from an extreme thermophile, *Thermus thermophilus* HB8. Acta Crystallogr D Biol Crystallogr **54:** 1032–1034

Nobe Y, Kawaguchi S, Ura H, Nakai T, Hirotsu K, Kato R, Kuramitsu S (1998) The novel substrate recognition mechanism utilized by aspartate aminotransferase of the extreme thermophile *Thermus thermophilus* HB8. J Biol Chem **273:** 29554–29564

Okamoto A, Higuchi T, Hirotsu K, Kuramitsu S, Kagamiyama H (1994) X-ray crystallographic study of pyridoxal 5′-phosphate-type aspartate aminotransferases from *Escherichia coli* in open and closed form. J Biochem **116:** 95–107

Pagnussat GC, Yu HJ, Ngo QA, Rajani S, Mayalagu S, Johnson CS, Capron A, Xie L-F, Ye D, Sundaresan V (2005) Genetic and molecular identification of genes required for female gametophyte development and function in Arabidopsis. Development **132:** 603–614

Reynolds PH, Smith LA, Dickson JM, Jones WT, Jones SD, Rodber KA, Carne A, Liddane CP (1992) Molecular cloning of a cDNA encoding aspartate aminotransferase-P2 from lupin root nodules. Plant Mol Biol **19:** 465–472

Rhee S, Silva MM, Hyde CC, Rogers PH, Metzler CM, Metzler DE, Arnone A (1997) Refinement and comparisons of the crystal structures of pig cytosolic aspartate aminotransferase and its complex with 2-methylaspartate. J Biol Chem **272:** 17293–17302

Riens B, Lohaus G, Heineke D, Heldt HW (1991) Amino acid and sucrose content determined in the cytosolic, chloroplastic, and vacuolar compartments and in the phloem sap of spinach leaves. Plant Physiol **97:** 227–233

Rodríguez-Caso C, Rodríguez-Agudo D, Moya-García A, Fajardo I, Medina MA, Subramaniam V, Sánchez-Jiménez F (2003) Local changes in the catalytic site of mammalian histidine decarboxylase can affect its global conformation and stability. Eur J Biochem **270:** 4376–4387

Sali A, Blundell TL (1993) Comparative protein modelling by satisfaction of spatial restraints. J Mol Biol **234:** 779–815

Schultz CJ, Coruzzi GM (1995) The aspartate aminotransferase gene family of Arabidopsis encodes isoenzymes localized to three distinct subcellular compartments. Plant J **7:** 61–75

Shen MY, Sali A (2006) Statistical potential for assessment and prediction of protein structures. Protein Sci **15:** 2507–2524

Taniguchi M, Kobe A, Kato M, Sugiyama T (1995) Aspartate aminotransferase isozymes in *Panicum miliaceum* L. and NAD-malic enzyme-type C4 plant: comparison of enzymatic properties, primary structures and expression patterns. Arch Biochem Biophys **318:** 295–306

Thompson JD, Higgins DG, Gibson TJ (1994) CLUSTAL W: improving the sensitivity of progressive multiple sequence alignment through sequence weighting, position-specific gap penalties and weight matrix choice. Nucleic Acids Res **22:** 4673–4680

Turano FJ, Weisemann JM, Matthews BF (1992) Identification and expression of a cDNA clone encoding aspartate aminotransferase in carrot. Plant Physiol **100:** 374–381

Ura H, Nakai T, Kawaguchi SI, Miyahara I, Hirotsu K, Kuramitsu S (2001) Substrate recognition mechanism of thermophilic dual-substrate enzyme. J Biochem **130:** 89–98

Wadsworth GJ (1997) The plant aminotransferase gene family. Physiol Plant **100:** 998–1006

Wadsworth GW, Marmaras SM, Matthews BF (1993) Isolation and characterization of a soybean cDNA clone encoding the plastid form of aspartate aminotransferase. Plant Mol Biol **21:** 993–1009

Weber A, Flügge UI (2002) Interaction of cytosolic and plastidic nitrogen metabolism in plants. J Exp Bot **53:** 865–874

Wendel JF, Weeden NF (1989) Visualization and interpretation of plant isoenzymes. *In* DE Soltis, PS Soltis, eds, Isoenzymes in Plant Biology. Dioscorides Press, Portland, OR, pp 5–45

Wilkie SE, Lambert R, Warren MJ (1996) Chloroplast aspartate aminotransferase from *Arabidopsis thaliana*: an examination of the relationship between the structure of the gene and the spatial structure of the protein. Biochem J **319:** 969–976

Wilkie SE, Roper JM, Smith AG, Warren MJ (1995) Isolation, characterisation and expression of a cDNA clone encoding plastid aspartate aminotransferase from *Arabidopsis thaliana*. Plant Mol Biol **27:** 1227–1233

Wilkie SE, Warren MJ (1998) Recombinant expression, purification, and characterization of three isoenzymes of aspartate aminotransferase from *Arabidopsis thaliana*. Protein Expr Purif **12:** 381–389

Winter H, Robinson DG, Heldt HW (1994) Subcellular volumes and metabolite concentrations in spinach leaves. Planta **193:** 530–535

Yagi T, Kagamiyama H, Nozaki M, Soda K (1985) Glutamate-aspartate transaminase from microorganisms. Methods Enzymol **113:** 83–89